QUALITATIVE ANALYSIS OF THE TEMPERATURE FIELD PRODUCED BY AN EARLY STAGE TUMOR

GABRIEL KACSO[1], IOAN FLOREA HĂNȚILĂ[2], OANA MIHAELA DROSU[2], MIHAI MARICARU[2], MARILENA STĂNCULESCU[2]

Key words: Pennes' equation, Analytical methods, Sensitivities, Breast tumor depth.

Modern versatile thermographical techniques have recently renewed the research direction for the early detection of the breast cancer. An unusual temperature field on the breast surface can be induced by the presence of a malignant tumor, due to a higher metabolism of the cancer cells comparing to the normal ones. Localising the tumor and determining its morphology based on the temperature field on the breast surface is an ill conditioned problem that needs a huge computation effort. We investigate the influence of the breast tissue thermal and geometric parameters on the surface temperature field. Also, some techniques for determining the affected area are commended. A simplified model of the breast geometry is adopted in order to obtain an analytical solution for Pennes' equation. The results are extremely useful for the analysis of the real breast geometry, drastically limiting the investigation area.

1. **INTRODUCTION**

The annual incidence of the breast cancer has increased lately, triggering an increased mortality caused by this disease [1], despite huge efforts of optimizing tailored individualized therapy. The early diagnosis of the disease remains the most effective way to increase the life span. Basically, this relies on the identification of the primary breast tumor at a very small size, e.g. around 5 mm, completely asymptomatic. The most commonly used methods for early detection of breast cancer are the ultrasound and mammography; MRI is recently getting increased popularity, but still remains cost prohibitive as screening tool.

A highly interesting technique is provided by examining the temperature field on the breast surface. The principle of the method is based on the fact that the cancer cells may have a much higher metabolism than the normal cell. In Table 1

[1] "Iuliu Haţieganu" University of Medicine and Pharmacy, 8 Babeş St., Cluj-Napoca, 400012, Romania, E-mail: gabi.kacso@gmail.com.

[2] "Politehnica" University of Bucharest, Department of Electrical Engineering, Spl. Independentei 313, Bucharest, 060042, Romania, E-mail: hantila@elth.pub.ro.

Rev. Roum. Sci. Techn.– Électrotechn. et Énerg., **59**, *4,* p. 433–443, Bucarest, 2014

[2] the specific caloric powers of the tumor *(SCP)*, according to its size are given. Interestingly, for small dimensions, the *SCP* of the tumor is very large compared to the glandular tissue (450 W/m^3). It would allow the detection of some breast cancers long before mammography (Table 2 [3,4]).

Table 1

SCP and p_{tum} of the tumor tissue

Tumor diameter (mm)	10	15	20	25	30
SCP (W/m^3)	65400	13600	8720	6827	5790
p_{tum} (W)	0.034226	0.024021	0.036508	0.055825	0.081813

Table 2

Diagnostic tools according to the number of tumor cells of a primary breast cancer

Years	1	2	3	4	5	6	7	8
No. of cells	16	256	4,096	65,536	1,048,576	16,777,216	268,435,456	4,294,967,296
Information obtained using		Thermography						
								Mammography

Some tumors are not detectable through mammography [5]. That doesn't mean necessarily that the thermography could replace totally the mammography. There are many benign diseases of the breast giving abnormal thermic field on the surface, inducing false-positive results; there are also false negative results due to measurements errors or to so called "cold" tumors. The diagnosis strategy can be improved by combining mammography with thermography.

The thermal field verifies Pennes' equations and the detection of tumor location and volume needs to solve an inverse, ill-conditioned problem. The finite element method with first degree elements on a tetrahedral mesh, has been used in [6] and [7], in order to solve the direct Pennes' problem. The tetrahedra in which the tumor is the most likely located has been searched. Procedures for fast calculation of the modified matrix have been proposed, taking into consideration the fact that the thermal parameters are modified only in the tetrahedra associated with tumor. However, the computation time is huge, due to the large number of trials.

If the thermal parameters of the breast tissue would have an important influence on the result of the thermal field problem, the inability to precisely determine these parameters and breast structure would make impossible the thermographic method to detect breast tumor location and size. Therefore it is particularly important to study the sensitivity of the temperature field on the surface of the breast in relation to these parameters. Given the great diversity of shapes of breasts, a simple configuration must be chosen, for the qualitative results to be credible. In [2] an axisymmetric configuration is proposed, where (in the cross section) the tissues are separated by circles and the tumor with circular shape and different diameters is placed at different depths. The problem can be solved

only numerically (COMSOL). In [8] a spherical geometry for breast is proposed; a paralelipipedical basement, representing the pectoral tissue is added and the results are also obtained using numerical methods.

In this paper, an axisymmetric cylindrical model has been proposed, for which analytical solutions can be obtained. In this way, changing parameters can be easily done and the solution is obtained very rapidly. The dependence of the temperature field on the breast surface is analyzed, modifying the cylinder geometry, the subcutaneous layer dimension, the tumor depth, the thermal conductivity and the blood perfusion coefficient. Having the analytical solutions, any other parameter can be easily changed. The purpose is to study the early tumors, assumed to have the shape of a Dirac impulse. Therefore the tumor dimension may be neglected. As consequence it can be admitted that there is no significant domain with tumor blood perfusion coefficient (as the neoangiogenesis is in his inception). In this way superposition can be applied. Some procedures for determining the depth and tumor dimensions have been recommended.

2. **THE METHOD**

2.1. THE ANATOMICAL MODEL

The chosen model for the analysis of the sensitivities is given in Fig. 1. For this model, the Pennes' equation in polar coordinates is

$$-\lambda\left(\frac{\partial^2 T}{\partial z^2}+\frac{\partial^2 T}{\partial r^2}+\frac{1}{r}\frac{\partial T}{\partial r}\right)+\gamma(T-T_b)=p\ , \tag{1}$$

where λ is thermic conductivity, $\gamma(T-T_b)$ represents the contribution of the blood flow to tissue heating, T_b is blood temperature, $\gamma = c_b w_b$ is blood perfusion coefficient (BPC), c_b is volumic thermal capacity of blood, w_b is the volume flow of the blood and p is the specific power of the tissue. The boundary conditions are: $\partial T/\partial r = 0$, for the symmetry axis $r = 0$; $T = T_e$, for $r = a$, a being the breast radius, where T_e is the temperature of the environment, $\lambda\partial T/\partial z = \alpha(T-T_e)$, for $z = 0$, $\lim_{z\to\infty} T(z,r) = T_b$, α beeing the equivalent thermal convection coefficient, that contains the effects of convection, radiation and evaporation.

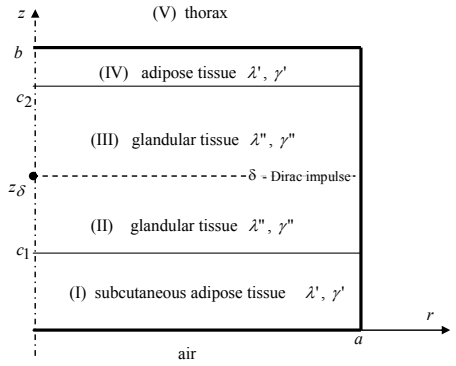

Fig.1 – The proposed model of the breast structure.

If the tissue is healthy (the tumor does not exist), then the temperature is T_0. This verifies the equation (1) and the boundary conditions. We suppose that at the point ($z = z_\delta$, $r = r_\delta$) a tumor appears as a Dirac impulse, which, in polar coordinates, represents a power

$$p_\delta = \frac{1}{2\pi r_\delta}\delta(r - r_\delta) \ . \tag{2}$$

The temperature of the body affected by the tumor $T_{dis} = T_0 + T_\delta$ verifies the equation (1) and the boundary conditions. It results that the temperature produced by the tumor T_δ, verifies the equation (1), but the boundary conditions are zero.

2.2. ANALYTICAL SOLUTION

Prof. C. Fluerasu presents in [9] how the separation of variables method can be applied for solving a Helmholtz problem with Dirac impulse sources. Our 2D thermal field is written in terms of Bessel eigenfunctions series and the transition condition in $z = z_\delta$ has a jump, describing the Dirac impulse. We express $T_\delta = Z(z)R(r)$ and for the areas *I, II, III, IV, V* we have

$$\frac{1}{Z}\frac{\mathrm{d}^2 Z}{\mathrm{d}z^2} + \frac{1}{R}\left(\frac{\mathrm{d}^2 R}{\mathrm{d}r^2} + \frac{1}{r}\frac{\mathrm{d}R}{\mathrm{d}r}\right) - \frac{\gamma}{\lambda} = 0. \tag{3}$$

Taking into consideration the zero boundary conditions, we obtain $\frac{1}{R}\left(\frac{\mathrm{d}^2 R}{\mathrm{d}r^2} + \frac{1}{r}\frac{\mathrm{d}R}{\mathrm{d}r}\right) = -\beta^2$ and $\frac{1}{Z}\frac{\mathrm{d}^2 Z}{\mathrm{d}z^2} = \sqrt{\beta^2 + \gamma/\lambda}$. Equation (3) has the solution

$$T_\delta(z,r)=\sum_k (A_k e^{-\eta_k z}+B_k e^{\eta_k z})J_0(\beta_k r)\ , \tag{4}$$

where x_k are the roots of the Bessel function J_0, $\beta_k = x_k / a$, and $\eta_k = \sqrt{\beta_k^2 + \gamma/\lambda}$. Applying the boundary condition for $z \to \infty$, it results that $B_k^V = 0$ for the area *V*. Between the areas IV and V for ($z = b$), we have $\lambda''\partial T_\delta^V / \partial z = \lambda'\partial T_\delta^{IV} / \partial z$ and $T_\delta^V = T_\delta^{IV}$, so

$$B_k^{IV} = A_k^{IV}\frac{\lambda'\eta_k' - \lambda''\eta_k''}{\lambda'\eta_k' + \lambda''\eta_k''}e^{-2\eta_k' b} = \Lambda_k A_k^{IV}\ , \tag{5}$$

where $\Lambda_k = -\Gamma_{k_2} e^{-2\eta_k' b}$, $s_k = \lambda''\eta_k'' + \lambda'\eta_k'$, $d_k = \lambda''\eta_k'' - \lambda'\eta_k'$, $\Gamma_{k_2} = -d_k / s_k$. From the boundary condition on $z = 0$, it results $B_k^I = \Gamma_{k_1} A_k^I$, where $\Gamma_{k_1} = \frac{\lambda'\eta_k' + \alpha}{\lambda'\eta_k' - \alpha}$. The transition conditions between areas I and II, for $z = c_1$, are: $T_\delta^{II} = T_\delta^I$ and $\lambda''\partial T_\delta^{II} / \partial z = \lambda'\partial T_\delta^I / \partial z$, thus

$$A_k^{II} = A_k^I \frac{s_k e^{-\eta_k' c_1} + \Gamma_{k_1} d_k e^{\eta_k' c_1}}{2\lambda''\eta_k'' e^{-\eta_k'' c_1}},\quad B_k^{II} = A_k^I \frac{d_k e^{-\eta_k' c_1} + \Gamma_{k_1} s_k e^{\eta_k' c_1}}{2\lambda''\eta_k'' e^{\eta_k'' c_1}}\ . \tag{6}$$

Between the areas III and IV, $T_\delta^{III} = T_\delta^{IV}$ for $z = c_2$ and $\lambda''\partial T_\delta^{III} / \partial z = \lambda'\partial T_\delta^{IV} / \partial z$, it results

$$A_k^{III} = A_k^{IV} \frac{s_k e^{-\eta_k' c_2} + \Lambda_k d_k e^{\eta_k' c_2}}{2\lambda''\eta_k'' e^{-\eta_k'' c_2}},\quad B_k^{III} = A_k^{IV} \frac{d_k e^{-\eta_k' c_2} + \Lambda_k s_k e^{\eta_k' c_2}}{2\lambda''\eta_k'' e^{\eta_k'' c_2}}\ . \tag{7}$$

Between the areas III and II, for $z = z_\delta$, a Dirac source is found, thus the transition conditions are: $T_\delta^{III} = T_\delta^{II}$ and $-\lambda''\left(\partial T_\delta^{III} / \partial z - \partial T_\delta^{II} / \partial z\right) = p_\delta$, so

$$A_k^{III} e^{-\eta_k'' z_\delta} + B_k^{III} e^{\eta_k'' z_\delta} = A_k^{II} e^{-\eta_k'' z_\delta} + B_k^{II} e^{\eta_k'' z_\delta}\ , \tag{8}$$

$$-\lambda''\sum_k \eta_k''\left(-A_k^{III} e^{-\eta_k'' z_\delta} + B_k^{III} e^{\eta_k'' z_\delta} + A_k^{II} e^{-\eta_k'' z_\delta} - B_k^{II} e^{\eta_k'' z_\delta}\right)J_0(\beta_k r) = \frac{1}{r_\delta}\delta(r - r_\delta)\ . \tag{9}$$

The equation (9) is multiplied by $rJ_0(\beta_k r)$, then integrated on [0, a] and for $r_\rho = 0$, we obtain

$$-A_k^{III} e^{-\eta_k'' z_\delta} + B_k^{III} e^{\eta_k'' z_\delta} + A_k^{II} e^{-\eta_k'' z_\delta} - B_k^{II} e^{\eta_k'' z_\delta} = -\frac{2}{a^2\lambda''\eta_k'' J_1^2(x_k)}\ . \tag{10}$$

From equations (5–8) and (10) the constants of Bessel functions series are found. The thermal field on the breast surface is

$$T_\delta^I(0,r)=\sum_k A_k^I(1+\Gamma_{k_1})J_0(\beta_k r)\ , \tag{11}$$

where

$$A_k^I=\frac{2\mathrm{e}^{-\eta_k' c_1}}{a^2 W_k J_1^2(x_k)}\Big[\mathrm{e}^{-\eta_k''(c_2-c_1)}\mathrm{e}^{-\eta_k''(c_2-z_\delta)}\left(d_k+\Gamma_{k_2}s_k\mathrm{e}^{-2\eta_k'(b-c_2)}\right)$$
$$+\mathrm{e}^{-\eta_k''(z_\delta-c_1)}\left(s_k+\Gamma_{k_2}d_k\mathrm{e}^{-2\eta_k'(b-c_2)}\right)\Big], \tag{12}$$

$$W_k=-\mathrm{e}^{-2\eta_k''(c_2-c_1)}\left(s_k\mathrm{e}^{-2\eta_k' c_1}+\Gamma_{k_1}d_k\right)\left(d_k+\Gamma_{k_2}s_k\mathrm{e}^{-2\eta_k'(b-c_2)}\right)$$
$$+\left(d_k\mathrm{e}^{-2\eta_k' c_1}+\Gamma_{k_1}s_k\right)\left(s_k+\Gamma_{k_2}d_k\mathrm{e}^{-2\eta_k'(b-c_2)}\right). \tag{13}$$

3. **RESULTS**

The analysis of the thermal field on the breast surface has been performed starting with the following data [10] (Fig. 1):

– thermic conductivities ($\mathrm{Wm^{-1}\,°C^{-1}}$) $\lambda'=0.21$, $\lambda''=0.48$;

– blood perfusion coefficients BPC ($\mathrm{Wm^{-3}\,°C^{-1}}$) $\gamma'=800$, $\gamma''=2400$;

– coordinates of the layers of subcutaneous and glandular tissues (all in mm): $c_1=8$, $c_2=46$, $b=50$, the position of the tumor is in the middle of the glandular tissue ($z_\delta=27$), breast radius $a=100$;

– the amplitude of Dirac impulse is given by the power $p=0.034226$ W of a tumor with 10 mm diameter (Table 1);

– thermal convection coefficient $\alpha=10$ W $\mathrm{°C^{-1}m^{-2}}$.

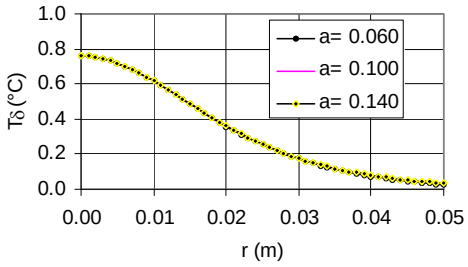

Fig. 2 – The influence of the radius a(m) on the temperature T_δ.

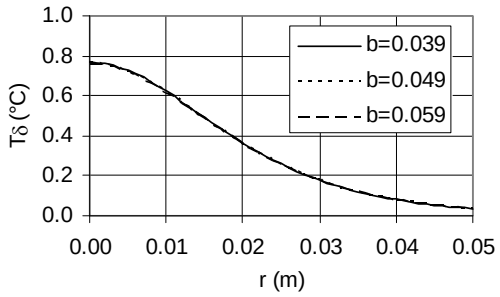

Fig. 3 – The influence of the breast thickness b(m) on the temperature T_δ.
Only the dimension c_2 was modified.

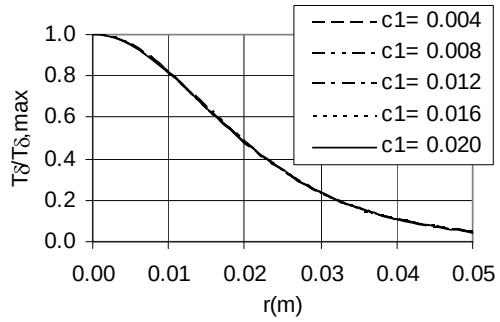

Fig. 4 – The influence of the breast subcutaneous tissue thickness c_1 (m)
on the relative temperature $T_\delta / T_{\delta,\max}$.

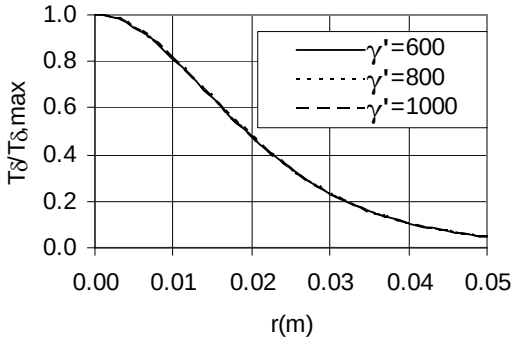

Fig. 5 – The influence of blood perfusion coefficient γ' ($\mathrm{Wm^{-3}/°C}$)
on the relative temperature $T_\delta / T_{\delta,\max}$.

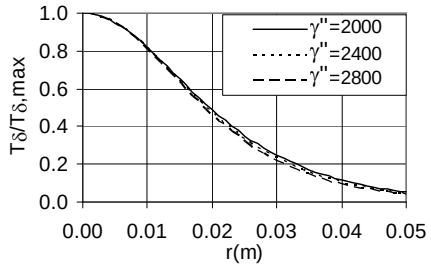

Fig. 6 – The influence of blood perfusion coefficient γ" ($Wm^{-3}/°C$) on the relative temperature $T_\delta / T_{\delta,\max}$.

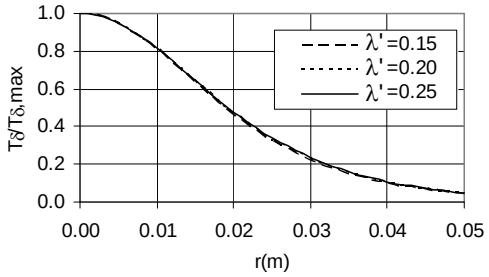

Fig. 7 – The influence of thermic conductivity λ' ($Wm^{-1}/°C$) of the subcutaneous tissue on the relative temperature $T_\delta / T_{\delta,\max}$.

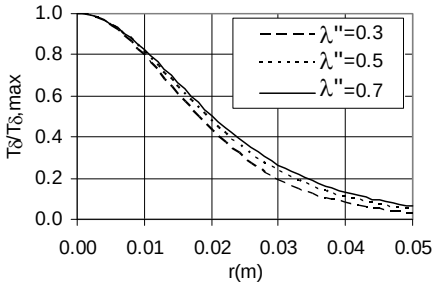

Fig. 8 – The influence of thermic conductivity λ" ($Wm^{-1}/°C$) of the tissue on the relative temperature $T_\delta / T_{\delta,\max}$.

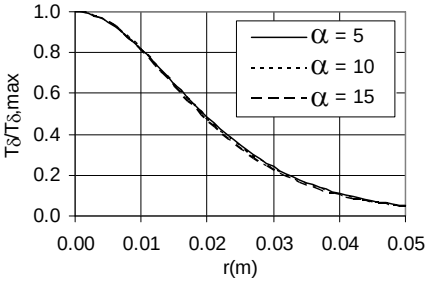

Fig. 9 – The influence of thermic convection coefficient α ($W m^{-2}/°C$) on the relative temperature $T_\delta / T_{\delta,\max}$.

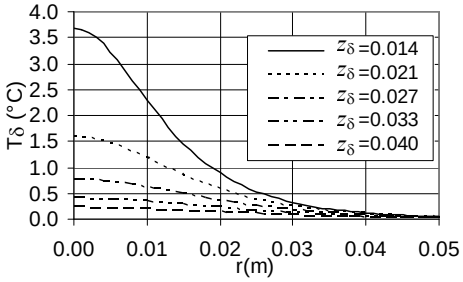

a) temperature T_δ .

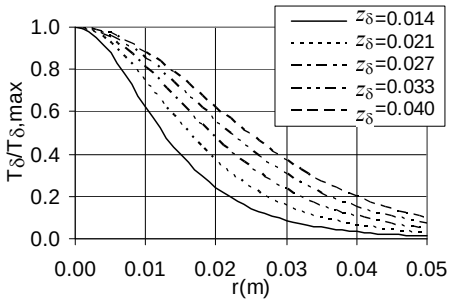

b) relative temperature $T_\delta / T_{\delta,\max}$.

Fig.10 – The influence of tumor depth z_δ (m) on the temperature field.

The changes of the temperature differences T_δ on the breast surface as a function of: breast radius a and breast thickness b are plotted in Fig. 2 and Fig. 3. The changes of the relative temperature differences $T_\delta / T_{\delta,\max}$ are described as a function of: the thickness c_1 of the subcutaneous tissue on the breast tissue (Fig. 4); the

blood perfusion coefficients γ_1 and γ_2 (Figs. 5, 6); the thermic conductivities λ_1 and λ_2 of the subcutaneous and glandular tissues (Figs. 7, 8); the thermic convection coefficient α on the breast surface (Fig. 9); the tumor depth (Fig. 10).

4. **COMMENTS**

The geometrical model adopted for breast structure can be justified by the fact that the radius and the thickness of the breast do not influence the field of the surface temperature (Figs. 2, 3).

The linearity of Pennes' equation, verified by the difference thermal field produced by a localised tumor having Dirac function shape, allows the application of superposition and, therefore, the graphics of the relative values $T_\delta / T_{\delta,\max}$ can be used. The shapes of the graphics $T_\delta / T_{\delta,\max}$ do not depend on the parameters c_1, γ_1, γ_2, λ_1, λ_2, α of the domain that was chosen for these parameters (Figs. 4–9).

Because only the depth z_δ of the tumor would have a great influence on the surface relative temperature $T_\delta / T_{\delta,\max}$ (Fig. 10), the others parameters being insignificant, it results that the shape of the graphic $T_\delta / T_{\delta,\max}$ can lead to an algorithm for localising the tumor. In Fig. 11 (dashed line) a graphic of the relative temperature $T_{mr,n}$ is presented, that can be measured in some points r_n and assumed to be affected by measurement errors. The depth of the tumor z_δ can be determined, minimising the error:

$$R(z_\delta) = \sum_n \left[T_\delta(r_n, z_\delta) / T_\delta(0, z_\delta) - T_{mr,n} \right]^2 . \tag{14}$$

Using the analytical expression of T_δ, the derivatives $\partial T_\delta / \partial z_\delta$ can be analytically determined and the equation $\mathrm{d}R(z_\delta)/\mathrm{d}z_\delta = 0$ can be rapidly solved. For the example given in Fig. 11, we obtain z_δ =0.02704925 m and the graphic of the relative temperature $T_\delta / T_{\delta,\max}$ corresponding to this depth (with continuous line).

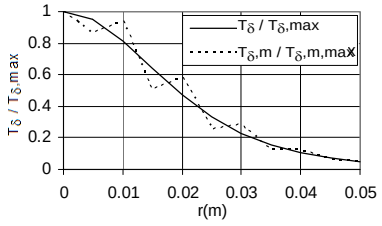

Fig. 11 – The measured and calculated relative temperatures for the same depth of the tumor.

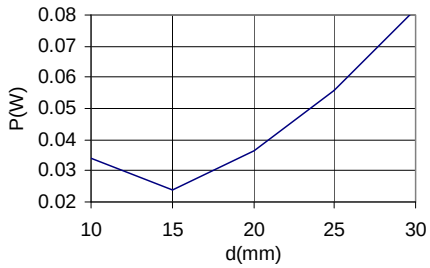

Fig. 12 – The dependence of the tumor power by the dimension *d* (Table I).

As the depth of the tumor is determined, the maximum measured temperature $T_{m,\max}$ is compared with the maximum calculated temperature $T_{\delta,\max}$ for a specific power p (in the case analysed in this paper: p = 0.034226 W) and the power of the tumor $P = p\,T_{m,\max}/T_{\delta,\max}$ is obtained. Unfortunately, if we consider the data of Table 1, given in [2], the dimensions of the tumor cannot be always determined (Fig. 12).

5. **CONCLUSIONS**

The paper has some important original contributions: 1) The Dirac impulse distribution adopted for the tumor shape is argued that especially early tumors detection is aimed and, specifically, it results the great advantage of the linearity of Pennes' equation. Consequently, the paper proposes the analysis of the relative temperature field $T_\delta / T_{\delta,\max}$ on the breast surface. 2) A simplified axisymmetric geometry is adopted for the breast shape. It is justified by the insignificant dependence of the surface temperature by the breast radius and thickness. The chosen model allows an analytical solution of the temperature field, based on which the influences of thermal and geometric parameters on temperature can be quickly analysed. Also, the derivative of the temperature with respect to this parameters may be easily performed. 3) The paper gives an important argument for the use of the thermic detection of the breast cancer: excepting the tumor depth, the influence of the geometric and thermic parameters on the relative temperature field is negligible. As a result, the tumor depth is determined with sufficient accuracy. The power of the tumor is quickly determined, due to the linearity of Pennes' equation.

For the real shape of the breast, the surface curvature can decrease the tumor depth with respect to that one determined in the paper. The great advantage is that, within a numerical search procedure, the search area is drastically reduced. We adopt for the tumor a specific size and power, then the search moves on the perpendicular direction on the surface of the breast from the point of maximum

temperature, starting with the depth determined according to the algorithm presented in the paper. The real depth of the tumor is determined comparing the calculated temperature field relative to the measured one. Then, around the obtained depth, the tumor size is modified until the calculated temperature is close to the measured one. (If case that the tumor is not a point, Pennes' equation is not linear anymore). A future paper will present the case of the real shape of the breast.

Received on June 30, 2014

REFERENCES

1. O. Suteu, N. Ghilezan, N. Todor, I. Petrache, *Epidemiologia cancerului de sân în România*, Revista Societății Române de Cancer – *Cancer, o provocare la viață*, **14**, 2006.
2. J. Kwok, J. Krzyspiak, *Thermal imaging and analysis for breast tumor detection*, BEE 453: Computer-Aided Engineering: Applications to Biomedical Processes, May 2007.
3. *** http://www.preventioniowa.com/pdf/thermography-brochure.pdf.
4. *** http://www.breastthermography.co.za/about.html.
5. R.D. Rosenberg, W.C. Hunt, et al., *Effects of age, breast density, ethnicity, and estrogen replacement therapy on screening mammographic sensitivity and cancer stage at diagnosis: review of 183,134 screening mammograms in Albuquerque, New Mexico*, Radiology, **209**, *2*, pp. 511–8, 1998.
6. F. Hantila, O. Drosu, M. Maricaru, *Breast tumour detection using the numerical analysis of the thermal inverse problem*, Journal of Optoelectronics and Advanced Materials, **10**, *5*, pp. 1295-1298, May 2008.
7. C. Tiu, F.I. Hantila, O. Drosu, M. Maricaru, A.S. Nica, *Localizing a breast tumor with thermographical methods*, SMIT 2008 Proceedings and MITAT, **17**, *4*, pp 209–245, 2008.
8. F.J. Gonzalez, *Thermal simulation of breast tumors*, Revista mexicana de fisica, **53**, *4*, pp. 323-326, 2007 (http://www.ejournal.unam.mx/rmf/no534/RMF005300414.pdf).
9. C. Fluerasu, *Electromagnetic field solution using the separation of variables method* (in Romanian), Lessons for Doctoral Students, Politehnica Institute of Bucharest, Department of Electrial Engineering, 1964.
10. E.Y. Ng, N.M. Sudharsan, *An improved three-dimensional direct numerical modelling and thermal analysis of a female breast with tumour*, Proceedings of the Institution of Mechanical Engineers. Part H; J. of Engineering in Medicine, **215**, *1*, pp. 25–37, 2001.